

The origin of the ferroelectric-like orthorhombic phase in oxygen-deficient HfO_{2-y} nanoparticles

Eugene A. Eliseev,^{1*} Hanna V. Shevilakova,² Oksana V. Leshchenko,¹ Victor N. Pavlikov,¹ Myroslav V. Karpets,¹ Lesya P. Yurchenko,¹ Yuri O. Zagorodniy,¹ Liubomyr M. Korolevych,² and Anna N. Morozovska^{3†}

¹Frantsevich Institute for Problems in Materials Science, National Academy of Sciences of Ukraine
Kyiv, Ukraine

²Department of Microelectronics Igor Sikorsky Kyiv Polytechnic Institute Kyiv, Ukraine

³Institute of Physics National Academy of Sciences of Ukraine Kyiv, Ukraine

Abstract — In this work, we present Landau-Ginzburg-Devonshire (LGD) model specifically an improved to describe charge-polarization coupling in the oxygen-deficient HfO_{2-y} nanoparticles. This model incorporates parametrized Landau expansion coefficients for both polar and antipolar orderings. To validate the model's accuracy, we utilized existing experimental X-ray diffraction data for the oxygen-deficient HfO_{2-y} nanoparticles (pure and doped with rare-earth elements). The X-ray diffraction confirmed the formation of a ferroelectric-like orthorhombic phase in the oxygen-deficient HfO_{2-y} nanoparticles, as well as in the HfO_{2-y} nanoparticles doped with the rare-earth element yttrium.

Keywords — nanoparticles, hafnia oxide, oxygen vacancies, rare-earth element doping, ferroelectric-like polar phase

INTRODUCTION

The discovery of ferroelectric and antiferroelectric properties in thin films of lead-free hafnium (HfO_2) and zirconium (ZrO_2) oxides open them for next-generation of Si-compatible ferroelectric memory elements like ferroelectric random-access memories (FeRAMs) and field-effect transistors (FETs) [1, 2]. However, a comprehensive understanding of the crucial interplay between stoichiometry, oxygen vacancies, size, and surface effects in nanosized $\text{Hf}_x\text{Zr}_{1-x}\text{O}_{2-y}$ remains elusive still.

This work aims to bridge this gap by investigating the charge-polarization coupling within these materials using the "effective" Landau-Ginzburg-Devonshire (LGD) model [3, 4, 5]. This approach leverages a limited number of polarization-field curves and hysteresis loops to parametrize the Landau expansion coefficients for polar (FE) and antipolar (AFE) orderings in hafnia-based compounds. To validate the effectiveness of the LGD model, we explain the X-ray diffraction data for oxygen-deficient HfO_{2-y} nanoparticles to determine their phase composition, as well as the nanoparticles prepared under varying annealing conditions (pure and doped with yttrium Y) and explain the formation of the ferroelectric-like orthorhombic phase in them.

Bulk HfO_2 and ZrO_2 , characterized as high-k dielectrics, lack inherent ferroelectric properties across a wide range of standard temperatures and pressures [6, 7]. This behavior undergoes a dramatic shift when these materials are scaled down to the nanoscale, where complex interactions and structural transitions come into play. One key factor influencing the observed ferroelectric properties in $\text{Hf}_x\text{Zr}_{1-x}\text{O}_2$ films is the presence of the polar orthorhombic phase. However, this phase suffers from metastability compared to the bulk monoclinic phase, leading to challenges with ferroelectric phase stability. Additionally, the properties of these thin films are highly sensitive to various factors, including substrate material, annealing conditions, deposition method, film thickness, and dopant concentrations [8, 9, 10]. Depending on the interplay of these

* Corresponding author: eugene.a.eliseev@gmail.com

† Corresponding author: anna.n.morozovska@gmail.com

factors, the value of x in $\text{Hf}_{1-x}\text{Zr}_x\text{O}_2$ films can range from 0 to 1, ultimately dictating whether the material exhibits dielectric, ferroelectric, or antiferroelectric behavior [11, 12].

Extensive theoretical [13, 14, 15] and experimental [16, 17, 18] theoretical and experimental evidence, as highlighted in our previous studies [3, 4, 5], underscores the critical role of surface and grain boundary energy, alongside oxygen vacancies, in optimizing these materials for practical applications in advanced FeRAM and FET technologies. Further research and optimization efforts are still required to fully unlock the full potential of binary oxide ferroelectric materials.

THE “EFFECTIVE” LANDAU-GINZBURG-DEVONSHIRE MODEL

Further analysis of the spatial-temporal evolution of polarization in the nanosized $\text{Hf}_x\text{Zr}_{1-x}\text{O}_{2-y}$ is conducted using a combined approach. This approach incorporates elements of the Kittel-type model[19], incorporating both polar and antipolar modes [20, 21, 22], with the theoretical framework of the Landau-Ginzburg-Devonshire (LGD) approach [3, 4, 5]. Within this framework, the free energy functional F is expressed as the sum of several key terms [3 - 5]:

$$F = F_{bulk} + F_{grad} + F_{el} + F_S. \quad (1)$$

The first term represents the bulk free energy, an expansion based on the second and fourth powers of both the polar (P_f) and antipolar (A_f) order parameters, F_{bulk} :

$$F_{bulk} = \int_{V_f} d^3r \left(\frac{a_P}{2} P_f^2 + \frac{b_P}{4} P_f^4 + \frac{\eta}{2} P_f^2 A_f^2 + \frac{a_A}{2} A_f^2 + \frac{b_A}{4} A_f^4 \right). \quad (2a)$$

Here V_f is the volume and surface area of the HfO_{2-y} nanoparticle. Subsequent terms account for the energy contribution arising from gradients in the polarization (F_{grad}), the electrostatic energy (F_{el}), and the surface energy (F_S), respectively are listed in Refs.[3 - 5].

It is important to consider how the LGD expansion coefficients depend on various factors, which in turn can be influenced by temperature, size, elastic stresses and/or strains. For classical ferroelectric films with a pronounced temperature-dependent and strain-dependent soft mode, the coefficients a_P and a_A exhibit a linear relationship with both temperature and strain (as shown in references (see [23, 24]).

Spatial-temporal evolution of P_f and A_f , is determined from the coupled time-dependent LGD type Euler-Lagrange equations, derived by minimizing the system's free energy F :

$$\Gamma_P \frac{\partial P_f}{\partial t} + a_P P_f + b_P P_f^3 + \eta A_f^2 P_f - g \Delta P_f = E_f, \quad (3a)$$

$$\Gamma_A \frac{\partial A_f}{\partial t} + a_A A_f + b_A A_f^3 + \eta P_f^2 A_f - g \Delta A_f = 0, \quad (3b)$$

where Γ_P and Γ_A are Landau-Khalatnikov relaxation coefficients [25], and g is a positive gradient coefficient written in an isotropic approximation. The relaxation times of P_f and A_f are $\tau_P = \Gamma_P/|a_P|$ and $\tau_A = \Gamma_A/|a_A|$, respectively. The corresponding boundary conditions for (3) are of the third kind [26]:

$$\left(P_f + \Lambda_P \frac{\partial P_f}{\partial n} \right) \Big|_S = 0, \quad \left(A_f + \Lambda_A \frac{\partial A_f}{\partial n} \right) \Big|_S = 0. \quad (4)$$

Here $\Lambda_P = \frac{g}{c_P}$ and $\Lambda_A = \frac{g}{c_A}$ are extrapolation lengths, which physical range is (0.5 – 5) nm [27]. Here S is the surface of the HfO_{2-y} nanoparticle.

Examples of how the effective LGD model works quantitatively are given in Refs.[3 - 5]. There polarization hysteresis loops, measured experimentally in $\text{Hf}_x\text{Zr}_{1-x}\text{O}_2$ thin films by Park et al. [11], are

shown The LGD-model parameters, determined from fitting of experimental results from Park et al. [11] in the references [3 - 5], are listed in the last four columns of **Table I**.

Table I. Landau-Ginsburg-Devonshire parameters of $\text{Hf}_x\text{Zr}_{1-x}\text{O}_2$ films*

x	phase	$P_r(x)$, C/m ²	$P_{c1,2}(x)$, C/m ²	$\tilde{\chi}(x)$	$a_p(x)$ $\times 10^9$, m/F	$a_A(x)$ $\times 10^9$, m/F	$b_p \approx b_A$ $\times 10^{10}$, Vm ⁵ /C ³	$\eta(x)$ $\times 10^{10}$, Vm ⁵ /C ³
0	PE	0	N/A	35	3.227	N/P	N/P	N/P
0.2	AFE	0	0.22, 0.17	40	0.812	-0.936	0.9	1.93
0.3	AFE	0	0.22, 0.15	50	0.010	-1.190	1.3	2.458
0.4	AFE	0	0.18, 0.11	48	-0.104	-0.937	1.1	2.888
0.50	FE	0.195	N/A	95	-0.594	N/P	1.563	N/P
0.57	FE	0.173	N/A	76	-0.743	N/P	2.483	N/P
0.70	FE	0.038	N/A	400	-0.141	N/P	10.039	N/P
0.81	PE	0.025	N/A	31	3.643	N/P	N/P	N/P
1.00	PE	0	N/A	19	5.944	N/P	N/P	N/P
<i>h</i>	films with thickness $h = 9.2$ nm							

*The content of Table I is licensed under a Creative Commons Attribution (CC BY) license (<https://creativecommons.org/licenses/by/4.0/>) in Supplementary Information to Ref. [<https://doi.org/10.1063/5.0209123>]

X-RAY DIFFRACTION FOR THE OXYGEN-DEFICIENT HfO_{2-y} NANOPARTICLES

To verify the model, we prepared several sample groups of stoichiometric HfO_2 , oxygen-deficient HfO_{2-y} and HfO_{2-y} doped nanoparticles doped with Y. Namely:

- **Sample group 1** annealed at 700°C for 6 hours (or more) in air,
- **Sample group 2** annealed at 600°C for 6 hours in air + 3,8 mol% of Y_2O_3 ,
- **Sample group 3** annealed at 500°C for 6 hours in $\text{CO}+\text{CO}_2$.

This diverse approach yielded samples with distinct color variations, reflecting differences in their oxygen vacancy concentrations, namely for Samples from 1 to 3 color changed from white to dark grey.

X-ray diffraction (XRD) analysis using an XRD-6000 diffractometer with $\text{Cu-K}\alpha_1$ radiation ($2\theta = 15-70^\circ$) and the database of the International Committee for Powder Diffraction Standards (JCPDS PDF-2) was used for identification the crystallographic phases of the HfO_2 nanoparticles. In the result, we confirmed the coexistence of both monoclinic and ferroelectric-like orthorhombic phases inside the oxygen-deficient nanoparticles. Namely, its significant amount has been found in sample groups 2 and 3 (see **Table II**). Notably, the relative abundance of each phase exhibited a demonstrably shifting pattern based on the specific annealing protocol employed, highlighting the sensitivity of phase composition to processing parameters.

Table II. XRD studies of HfO_{2-y} nanopowder sample groups

Sample group №	Phase	Mass fraction, %	Scattering region sizes, nm	Lattice parameters		
				<i>a</i> , Å	<i>b</i> , Å	<i>c</i> , Å
1	m	100	13	5,1220	5,1603	5,3025
2	m	16,85	11	5,1408	5,1771	5,4113
	o61	83,15	7	10,1180	5,1353	5,1583
3	m	13,24	12	5,1250	5,1580	5,3048

	o61	86,76	8	10,1089	5,2076	5,1202
--	-----	-------	---	---------	--------	--------

XRD analysis revealed a progressive shift in the sample's phases with changing annealing conditions. A Sample group 1 has the pure monoclinic phase ("m") as should be for a stoichiometric HfO₂ nanopowder. The fraction of non-ferroelectric monoclinic phase ("m") decreased from 100% (for the sample group 1) to 13.24% (for the sample group 3), while the ferroelectric-like orthorhombic phase ("o61") increased from 0% (for the sample group 1) to 86.76% (for the sample group 3), respectively. The progressive change in the phase composition, namely increasing of the ferroelectric-like orthorhombic phases, is attributed to the rise in oxygen vacancy concentration induced by the specific annealing conditions and/or rare-earth doping. Corresponding XRD spectra of oxygen-deficient HfO_{2-y} nanopowders are shown in **Fig. 1** and **Fig. 2**, respectively.

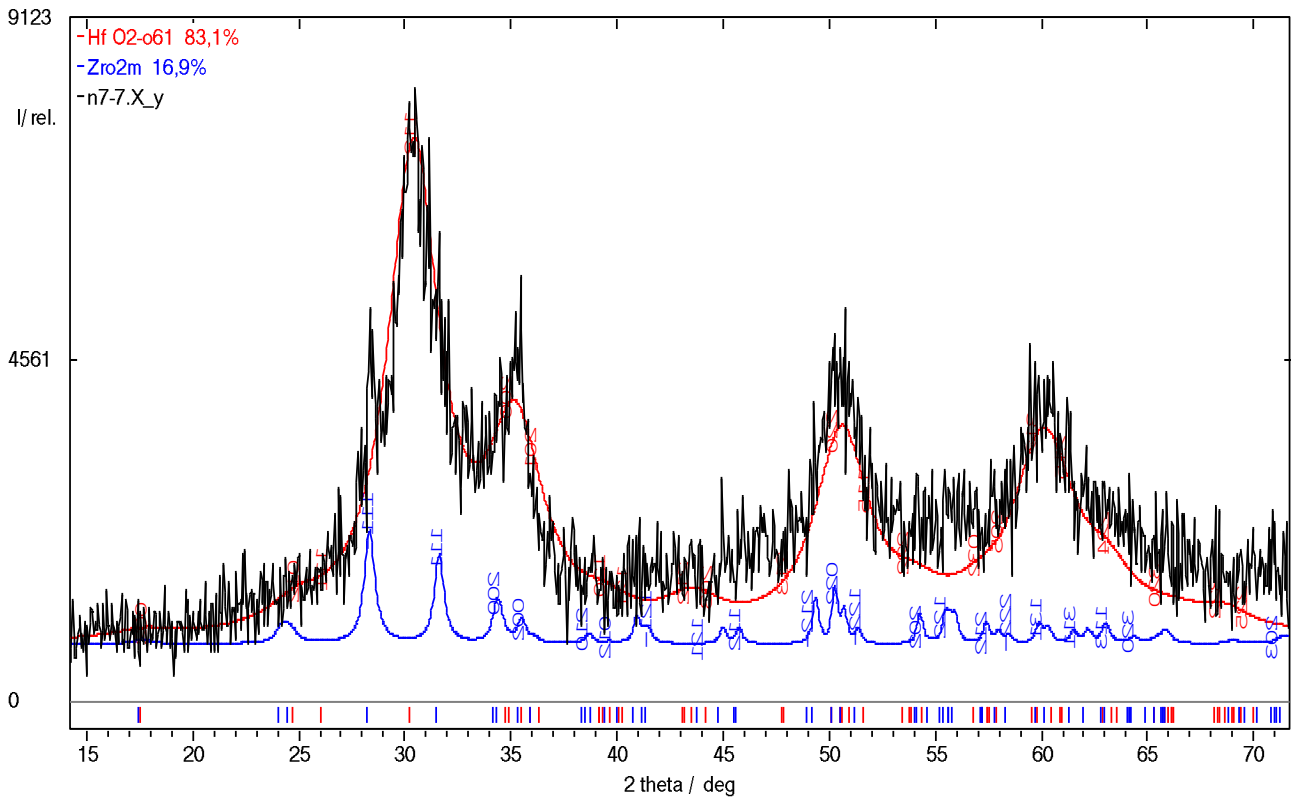


Figure 1. XRD spectra of oxygen-deficient HfO_{2-y} nanopowders annealed at 600°C for 6 hours in air under the presence of 3,8 mol% of Y₂O₃

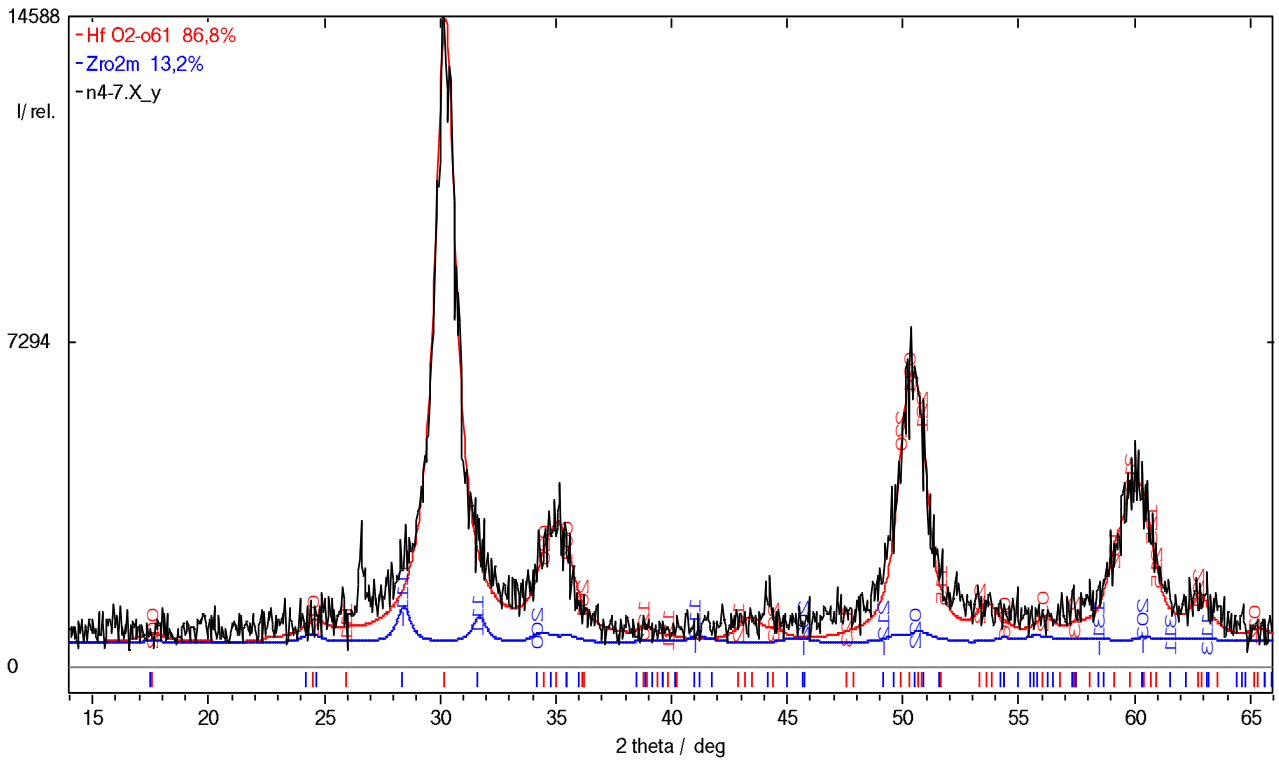


Figure 2. XRD spectra of oxygen-deficient HfO_{2-y} nanopowders annealed at 500°C for 6 hours in $\text{CO}+\text{CO}_2$ atmosphere

This comprehensive dataset, along with the sizes of the coherent scattering regions, forms foundation for the subsequent verification of the proposed effective Landau-Ginzburg-Devonshire (LGD) model.

EFFECTIVE LGD MODEL FOR OXYGEN-DEFICIENT HfO_{2-y} NANOPARTICLES

Using the phase fractions and coherent scattering region sizes obtained from XRD (**Table II**), we employ the effective LGD model to simulate stoichiometric and oxygen-deficient HfO_2 nanoparticles. The model incorporates a vacancy concentration gradient, mimicking the presumed distribution, as shown in **Fig. 3(a)**.

These vacancies act as elastic dipoles, influencing the material's stability. The calculated polarization-field hysteresis loops (shown in **Fig. 3(b)**) reveal a progressive transition from dielectric-like to antiferroelectric and ferroelectric characteristics with increasing vacancy concentration, aligning well with the experimental XRD findings.

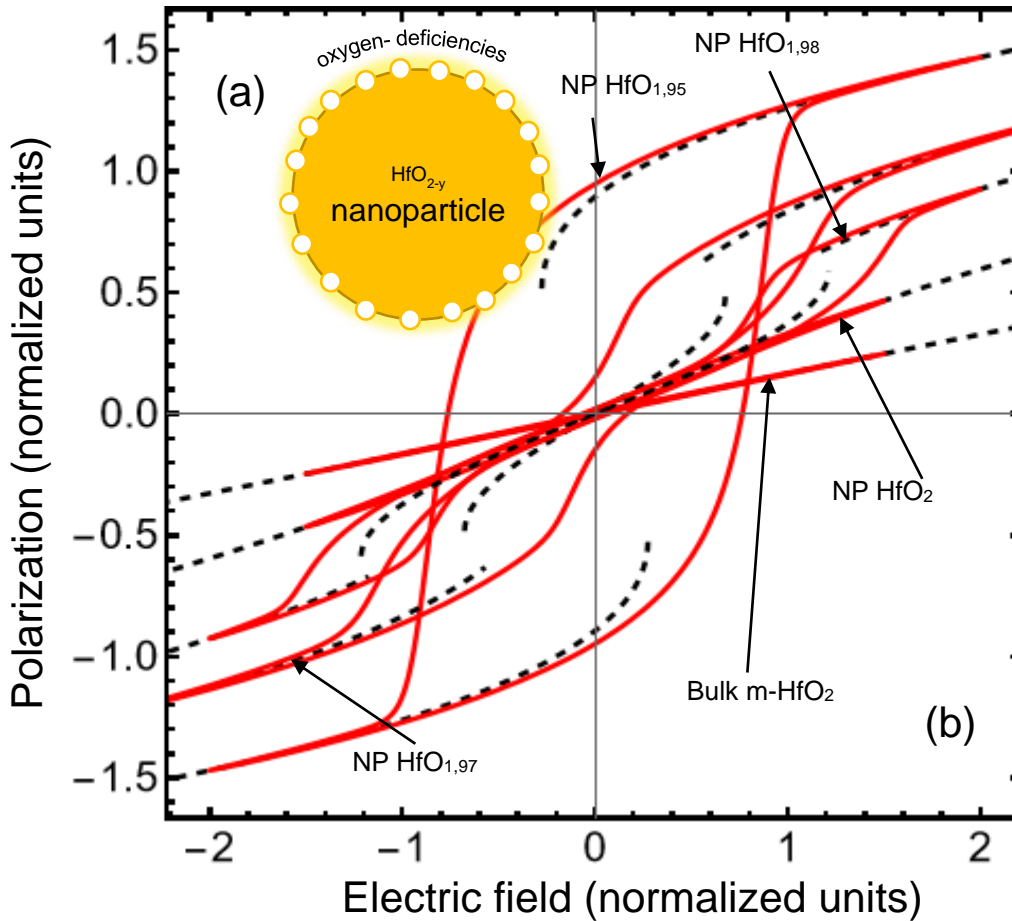


Figure 3. (a) The radial cross-section of the oxygen-deficient HfO_{2-y} nanoparticle. (b) Polarization-field dependences (hysteresis loops) calculated using the effective LGD model for the stoichiometric HfO_2 bulk, 20-nm size stoichiometric HfO_2 nanoparticles (NP) and HfO_{2-y} nanoparticles with different concentration of oxygen vacancies near the surface: $y = 2\%$, 3% and 5% . The dielectric-type, paraelectric-type, antiferroelectric-type and ferroelectric-type loops are shown. Black dotted curves show the equilibrium polarization-field dependences and red solid curves show the dynamic polarization-field hysteresis loops.

CONCLUSIONS

Our research delves into the intricate relationship between charge and polarization in nanoscale $\text{Hf}_x\text{Zr}_{1-x}\text{O}_{2-y}$ materials. To achieve this, we have refined the effective Landau-Ginzburg-Devonshire (LGD) model [3-5] through a tailored parameterization approach, specifically focusing on the Landau expansion coefficients associated with polar (FE) and antipolar (AFE) orderings.

To validate our refined model, we leveraged existing experimental data from $\text{Hf}_x\text{Zr}_{1-x}\text{O}_{2-y}$ thin films and oxygen-deficient HfO_{2-y} nanoparticles. Notably, X-ray diffraction (XRD) analysis of these materials confirmed the formation of the ferroelectric orthorhombic phase.

This successful application of the refined LGD model opens exciting avenues for the development of a novel generation of silicon-compatible ferroelectric nanomaterials based on $\text{Hf}_x\text{Zr}_{1-x}\text{O}_{2-y}$. This holds immense potential for future advancements in the field of nanotechnology and material science.

Authors' contribution

The research idea belongs to E.A.E., A.N.M. and Y.O.Z. E.A.E. wrote the codes, performed numerical calculations and compared with experiments. O.V.L., V.N.P., L.P.Y., Y.O.Z. and M.V.K. prepared the samples and performed XRD measurements. A.N.M. and H.V.S. wrote the manuscript draft. All co-authors analyzed the obtained results.

Acknowledgment

The work of E.A.E., L.P.Y. and Y.O.Z. and are funded by the National Research Foundation of Ukraine (project "Silicon-compatible ferroelectric nanocomposites for electronics and sensors", grant N 2023.03/0127). The work of A.N.M. is supported by the Ministry of Science and Education of Ukraine (grant № PH/ 23 - 2023, "Influence of size effects on the electrophysical properties of graphene-ferroelectric nanostructures") at the expense of the external aid instrument of the European Union for the fulfillment of Ukraine's obligations in the Framework Program of the European Union for scientific research and innovation "Horizon 2020".

REFERENCES

- 1 T. Mikolajick, S. Slesazek, H. Mulaosmanovic, M. H. Park, S. Fichtner, P. D. Lomenzo, M. Hoffmann, U. Schroeder. Next generation ferroelectric materials for semiconductor process integration and their applications, *J. Appl. Phys.* 129, 100901 (2021), <https://doi.org/10.1063/5.0037617>
- 2 K.-H. Kim, I. Karpov, R. H. Olsson III, D. Jariwala. Wurtzite and fluorite ferroelectric materials for electronic memory, *Nature Nanotechnology* 18, 422 (2023). <https://doi.org/10.1038/s41565-023-01361-y>
- 3 A. N. Morozovska, M. V. Strikha, K. P. Kelley, S. V. Kalinin, and E. A. Eliseev. Effective Landau-type model of a $\text{Hf}_x\text{Zr}_{1-x}\text{O}_2$ -graphene nanostructure, *Phys. Rev. Applied* 20, 054007 (2023) <https://doi.org/10.1103/PhysRevApplied.20.054007>
- 4 E. A. Eliseev, Y. O. Zagorodniy, V. N. Pavlikov, O. V. Leshchenko, H. V. Shevilakova, M. V. Karpec, A. D. Yaremkevych, O. M. Fesenko, S. V. Kalinin, and A. N. Morozovska. Phase diagrams and polarization reversal in nanosized $\text{Hf}_x\text{Zr}_{1-x}\text{O}_{2-y}$, *AIP Advances*, 14, 055224 (2024), <https://doi.org/10.1063/5.0209123>
- 5 E. A. Eliseev, S. V. Kalinin, A. N. Morozovska. Ferro-ionic States and Domains Morphology in $\text{Hf}_x\text{Zr}_{1-x}\text{O}_2$ Nanoparticles (2024), <https://doi.org/10.48550/arXiv.2410.04476>
- 6 G. A. Kourouklis, and E. Liarokapis. Pressure and temperature dependence of the Raman spectra of zirconia and hafnia. *Journal of the American Ceramic Society* 74, 520 (1991), <https://doi.org/10.1111/j.1151-2916.1991.tb04054.x>
- 7 M. Ishigame, and T. Sakurai. Temperature dependence of the Raman spectra of ZrO_2 . *Journal of the American Ceramic Society* 60, 367 (1977), <https://doi.org/10.1111/j.1151-2916.1977.tb15561.x>
- 8 T.S. Boscke, S. Teichert, D. Brauhaus, J. Muller, U. Schroder, U. Bottger, and T. Mikolajick, Phase transitions in ferroelectric silicon doped hafnium oxide, *Appl. Phys. Lett.* 99, 112904 (2011), <https://doi.org/10.1063/1.3636434>.
- 9 Yu Yun, P. Buragohain, M. Li, Z. Ahmadi, Y. Zhang, X. Li, H. Wang, J. Li, P. Lu, L. Tao, H. Wang, Intrinsic ferroelectricity in Y-doped HfO_2 thin films, *Nature Materials*, 21, 903 (2022), <https://doi.org/10.1038/s41563-022-01282-6>
- 10 F. Delodovici, P. Barone, and S. Picozzi. Finite-size effects on ferroelectricity in rhombohedral HfO_2 . *Phys. Rev. B* 106, 115438 (2022), <https://doi.org/10.1103/PhysRevB.106.115438>
- 11 M. H. Park, Y. H. Lee, H. J. Kim, T. Schenk, W. Lee, K. Do Kim, F. P. G. Fengler, T. Mikolajick, U. Schroeder, and C. S. Hwang. Surface and grain boundary energy as the key enabler of ferroelectricity in

nanoscale hafnia-zirconia: a comparison of model and experiment. *Nanoscale* 9, 9973 (2017), <https://doi.org/10.1039/C7NR02121F>

12 D. Hyun Lee, Y. Lee, K. Yang, J.Y. Park, S.H. Kim, P.R.S. Reddy, M. Materano, H. Mulaosmanovic, T. Mikolajick, J.L. Jones, U. Schroeder, M.H. Park, Domains and domain dynamics in fluorite-structured ferroelectrics *Appl. Phys. Rev.* 8, 021312 (2021), <https://doi.org/10.1063/5.0047977>

13 L.-Y. Ma and S. Liu. Structural Polymorphism Kinetics Promoted by Charged Oxygen Vacancies in HfO₂ *Phys. Rev. Lett.* 130, 096801 (2023), <https://doi.org/10.1103/PhysRevLett.130.096801>

14 M.D. Glinchuk, A.N. Morozovska, A. Lukowiak, W. Stręk, M.V. Silibin, D.V. Karpinsky, Y.Kim, and S.V. Kalinin.. Possible Electrochemical Origin of Ferroelectricity in HfO₂ Thin Films. *Journal of Alloys and Compounds*, 830, 153628 (2020), <https://doi.org/10.1016/j.jallcom.2019.153628>

15 S. Kang, W.-S. Jang, A. N. Morozovska, O. Kwon, Y. Jin, Y.H. Kim, H. Bae, C. Wang, S.H. Yang, A. Belianinov, and S. Randolph, Highly enhanced ferroelectricity in HfO₂-based ferroelectric thin film by light ion bombardment. *Science*, 376, 731-738 (2022), <https://doi.org/10.1126/science.abk3195>

16 W. Yang, C. Yu, H. Li, M. Fan, X. Song, H. Ma, Z. Zhou, P. Chang, P. Huang, F. Liu, X. Liu, J. Kang. Ferroelectricity of hafnium oxide based materials: Current statuses and future prospects from physical mechanisms to device applications. *Journal of Semiconductors* 44, 1-45 (2023), <https://doi.org/10.1088/1674-4926/44/5/053101>

17 M. H. Park, C.-C. Chung, T. Schenk, C. Richter, K. Opsomer, C. Detavernier, C. Adelman, J.L. Jones, T. Mikolajick, U. Schroeder. Effect of Annealing Ferroelectric HfO₂ Thin Films: In Situ, High Temperature X-Ray Diffraction. *Advanced Electronic Materials* 4, 1800091 (2018), <https://doi.org/10.1002/aelm.201800091>

18 K. P. Kelley, A. N. Morozovska, E. A. Eliseev, Y. Liu, S. S. Fields, S. T. Jaszewski, T. Mimura, J. F. Ihlefeld, S. V. Kalinin. Ferroelectricity in Hafnia Controlled via Surface Electrochemical State. *Nature Materials* 22, 1144 (2023) <https://doi.org/10.1038/s41563-023-01619-9>

19 R. Blinc, B. Zeks, *Soft Mode in Ferroelectrics and Antiferroelectrics*; North-Holland Publishing Company, Amsterdam, Oxford, 1974.

20 A. K. Tagantsev, K. Vaideeswaran, S. B. Vakhrushev, A. V. Filimonov, R. G. Burkovsky, A. Shaganov, D. Andronikova, A. I. Rudskoy, A. Q. R. Baron, H. Uchiyama, D. Chernyshov, A. Bosak, Z. Ujma, K. Roleder, A. Majchrowski, J.-H. Ko & N. Setter. The Origin of Antiferroelectricity in PbZrO₃. *Nature Commun.* 4, article number: 2229 (2013), <https://doi.org/10.1038/ncomms3229>.

21 K.M. Rabe, *Antiferroelectricity in Oxides: A Reexamination*. In *Functional Metal Oxides*; John Wiley & Sons, Ltd; pp 221–244. <https://doi.org/10.1002/9783527654864.ch7> .

22 J. Hlinka, T. Ostapchuk, E. Buixaderas, C. Kadlec, P. Kuzel, I. Gregora, J. Kroupa, M. Savinov, A. Klic, J. Drahokoupil, I. Etxebarria, and J. Dec. Multiple Soft-Mode Vibrations of Lead Zirconate. *Phys. Rev. Lett.* 112, 197601 (2014). <https://doi.org/10.1103/PhysRevLett.112.197601>.

23 A. Tagantsev, L.E. Cross, J. Fousek, *Domains in Ferroic Crystals and Thin Films*; Springer: New York, 2010. 10.1007/978-1-4419-1417-0

24 A. Kvasov and A.K. Tagantsev. Role of high-order electromechanical coupling terms in thermodynamics of ferroelectric thin films. *Phys. Rev. B* 87, 184101 (2013), <https://doi.org/10.1103/PhysRevB.87.184101>.

25 L. D. Landau, and I. M. Khalatnikov. "On the anomalous absorption of sound near a second order phase transition point." *Dokl. Akad. Nauk SSSR*, vol. 96, pp. 469-472 (1954).

26 R. Kretschmer and K.Binder. "Surface effects on phase transitions in ferroelectrics and dipolar magnets." *Phys. Rev. B* 20, 1065 (1979), <https://doi.org/10.1103/PhysRevB.20.1065>.

27 Chun-Lin Jia, Valanoor Nagarajan, Jia-Qing He, Lothar Houben, Tong Zhao, Ramamoorthy Ramesh, Knut Urban & Rainer Waser, "Unit-cell scale mapping of ferroelectricity and tetragonality in epitaxial ultrathin ferroelectric films." *Nature Materials* 6, 64 (2007), <https://doi.org/10.1038/nmat1808>.